**References**

[1] H. Salmang, H. Scholze, R. Telle (ed.): Keramik. Springer, Berlin, Heidelberg (2007)

[2] W. Lan, P. Xiao: Drying stress of yttria-stabilized-zirconia slurry on a metal substrate. J. European Ceramic Soc. 27 (2007) 3117-3125

[3] X. Wang, W.H. Lan, P. Xiao: Fabrication of yttria stabilized zirconia coatings by a novel slurry method. Thin Solid Films 494 (2006) 263-267

[4] M. Aslan, J. Adam, B. Reinhard, M. Veith: Preparation of thick zirconia coatings by spraying of colloidal suspensions. Proceedings of the 10th International Conference and Exhibition of the European Ceramic Society, 17.-21. June 2007 in Berlin

[5] M.J.M. Akash: Zr surface diffusion in tetragonal yttria stabilised zirconia. J. Materials Science 35 (2000) 437-442

[6] G. Skandan: Processing of nanostructured zirconia ceramics. NanoStructured Materials 5 (1995) 111-126

[7] W. Li, L. Gao: Compacting and sintering behaviour of nano ZrO2 powders. Scripta materialia 44 (2001) 2269-2272

[8] J. Rankin, B.W. Sheldon: In situ TEM sintering of nano-sized ZrO2 particles. Materials Science and Engineering A204 (1995) 48-53

[9] E. Mamontov: Dynamics of surface water in ZrO2 studied by quasielastic neutron scattering. J. Chemical Physics 121 (2004) 9087-9097

[10] G. Cerrato, S. Bordiga, S. Barbera, C. Morterra: Surface characterization of monoclinic ZrO2, I. Morphology, FTIR spectral features, and computer modelling. Applied Surface Science 115 (1997) 53-65

[11] H. Schmidt, K.-P. Schmitt, K. Schmitt, F. Tabellion: Method for production of nanoparticles with custom surface chemistry and corresponding colloids. Patent application WO 2006037591 A3 (priority: 2004)

# Preparation of Acoustic Lenses by Mechanochemical Synthesis and Electrophoretic Deposition of Lead Zirconium Titanate (PZT) Films

(*): IBMT - Fraunhofer-Institut für Biomedizinische Technik, 66386 St. Ingbert

**Abstract**

PZT powder has been synthesized via reactive dry milling using $PbZrO_3$ and $PbTiO_3$ as starting materials. Stable suspensions of the PZT particles in ethanol ($d_{50}$(Vol) = 115 nm) were obtained by a chemomechanical disper-

sion step. The electrophoretic deposition has been optimized varying the cell voltage and the PZT solid content in the suspension. PZT films have been deposited on platinum coated sapphire. After drying, the films are densely packed and free of cracks. By using lithium acetate and lead acetate as a sinter aid it was possible to reduce the sintering temperature to 1050°C. A gold electrode has been sputtered onto the piezolectric films which then have been poled by the corona method. The circular PZT dots (Ø = 2 mm) with a thickness of 1 µm show the expected oscillation resonance at about 2 GHz and can be used in acoustic lenses, for example in acoustic microscopes.

**Introduction**

In liquids acoustic waves in the gigahertz range are known to have wavelengths comparable to that of visible light [1]. In acoustic microscopy this property is used to determine the elastic structure of samples in a mechanical scanning system.

The basic component in an acoustic microscope is the acoustic lens. This is a simple device made of a single-crystal silicon-substrate supporting the piezoelectric unit which is composed of the piezoelectric ceramic (mostly ZnO) and two electrodes [1]. The working-frequency of the lense depends on the thickness of the ceramic layer.

The piezoelectric properties of PZT (stoichiometry in this work: $Pb(Zr_{0.52}Ti_{0.48})O_3$ exceed the ones of ZnO. So the coupling factor of PZT is higher by a factor of 3 than that of ZnO [2]. The piezoelectric constant $d_{33}$ is higher about a factor of 10 [3].

So it should be promising to replace the ZnO ceramic by a PZT ceramic to make the advantages of PZT available for acoustic microscopy. In this work an acoustic lense, in which a piezoelectric PZT-ceramic is built by electrophoretic deposition (EPD), has been produced. EPD is chosen because of the easy process control in comparison to sputtering or chemical vapour deposition of PZT. Via EPD, stoichiometry and phase purity of the end-product is already fixed before the deposition process.

In the EPD-process it is possible to create highly uniform ceramic films [11]. Electrophoretic shaping is suitable for handling powders in the nanometer-range, since deposition velocity is independent from particle size. An adequately stabilised suspension of the particles is a precondition for a successful deposition. The stability of colloidal suspensions is described by the DLVO-theory [12, 13], labelled by Derjaguin, Landau, Verwey and Overbeek. According to that theory surfaces of colloidal particles are regarded as capacitor plates. In a suspension, electrochemical double layers form at the capacitor's surfaces. The range of the resulting repulsive forces is higher than the range of the attractive Van-der-Waals forces, which leads to a stabilization of the suspension.

Due to an applied electric field, charged particles in the suspension move to the

oppositely charged electrode, where they agglomerate to a dense green film. This green film has to be sintered to high densities and to be poled to make it suitable for sensors and actuators.

**Experimental**

The PZT powder used in this work is synthesised by a mechanochemical process. In a high energy ball mill provided with a jar (125 ml) and balls made of tungsten-carbide, commercially available $PbZrO_3$ (Aldrich) and $PbTiO_3$ (Aldrich) powders with a particle size distribution in the sub-µm-range are mechanochemically treated to get a single phase PZT-powder with a stoichiometry of $Pb(Zr_{0.52}Ti_{0.48})O_3$, which is near the morphotropic phase boundary. To determine optimal parameters for the mechanochemical process, rotation velocity, ball-to-powder weight ratio and rotation time are varied. The phase transition to PZT is observed by an X-ray diffractometer (Siemens D500). In previous works different conditions are described to get PZT by mechanochemical treatment [4, 5].

After the mechanochemical synthesis of the powders, the particles are strongly aggregated. So, a further chemomechanical dispersion step is applied. This step is accomplished in a laboratory ball mill (Fritsch, Pulverisette 6) with a $ZrO_2$-jar and $ZrO_2$-balls with 0.3 mm diameter in ethanol charged with an organic surface modifier, an oxocarboxylic acid. In using a carboxylic acid, among electrostatic stabilisation as described in the DLVO-theory, a steric stabilisation by the carbon chains is given. This combination is known as electrosteric stabilisation. In this way, the particles are deaggregated in a stabilized PZT/ethanol-suspension for use in the electrophoretic deposition process. Ethanol is used as dispersion medium because of experiences made by Ma [8, 9, 10]. The particle size distribution is determined by an ultrafine particle analyzer (UPA 400, Grimm). Further on the particles are characterized by SEM and EDX (JEOL, JSM 6400 F).

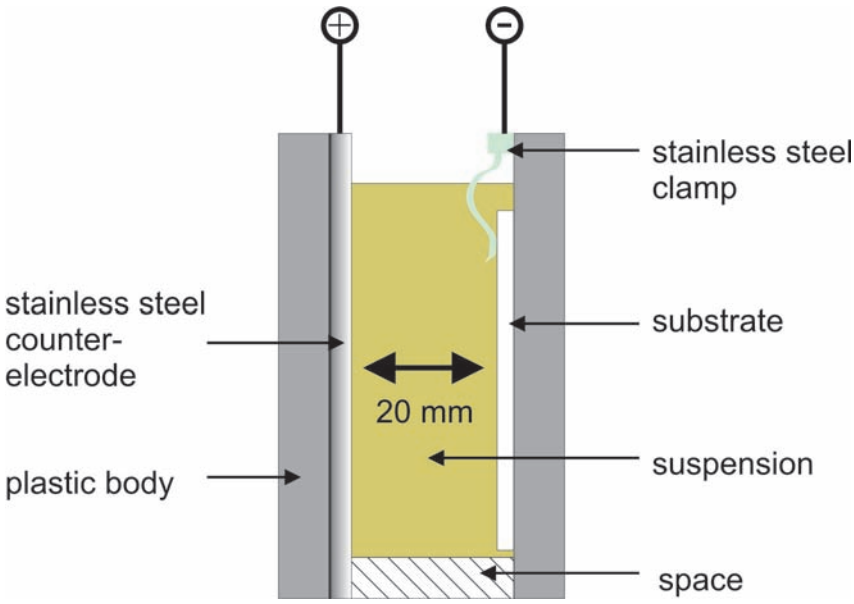


Fig. 1: EPD-cell.

16 short-circuited bottom-electrodes made of platinum are sputtered on to the sapphire-substrates. To avoid flaking of the electrodes during the sintering a sputtered 10 nm adhesive layer between substrate and platinum electrodes is used. The dimensions of the substrates are 5 cm x 5 cm x 2 mm. The resulting

Pt-dots have a diameter of 5 mm and a thickness of 200 nm – 1 µm. For use in acoustic microscopy, the thickness of the electrodes should be as low as possible to avoid loss of sonic energy.

To optimise the electrophoretic process, it is necessary to vary the cell voltage, the solid content in the suspension and the deposition time. The ζ-potential of the PZT-suspensions are measured at various pH values adjusted by NaOH and the surface modifier, an oxocarboxylic acid. After that, the pH has to be regulated to the maximum value of the ζ-potential to get a stabilized suspension. The design of the EPD-cell is shown in Figure 1. The substrate with the short-circuited electrodes is fixed and electrically contacted by a stainless-steel clamp. The metrics of the counter electrode made of stainless-steel are 80 mm x 50 mm x 2 mm. The distance of the electrodes is fixed at 20 mm. The cell is connected to a DC voltage source, counter electrode at positive pole, substrate at negative pole.

After deposition, green films are treated with a sintering aid. Van Tassel and Randall propose a sintering aid made of methyl ethyl ketone containing lead ethylhexanoate and lithium acetate with a small addition of methanol to dissolve the acetate [6]. In this work a similar aid is used made of lithium acetate-dihydrate, lead acetate-dihydrate, methyl ethyl ketone and methanol.

Sintering is accomplished in a cement sealed $Al_2O_3$-crucible with a lead-source to avoid the loss of lead in the PZT-film during the sintering process. Lead-source is a commercially available PZT-Powder (EPC, Ltd., PZT 856). The influence of the sintering aid is determined by a dilatometer and by SEM-images (JEOL, JSM 6400 F).

After the sintering process the top-electrode made of gold is sputtered on the PZT-films and the films are poled using the corona-method [7]. Now the functionalised coatings are ready to be characterised in a network analyzer (Hewlett Packard, HP 8719D). The analyzer generates a microwave-signal, which is supplied into a coaxial cable enclosed by the sample. The configuration is shown in Figure 2.

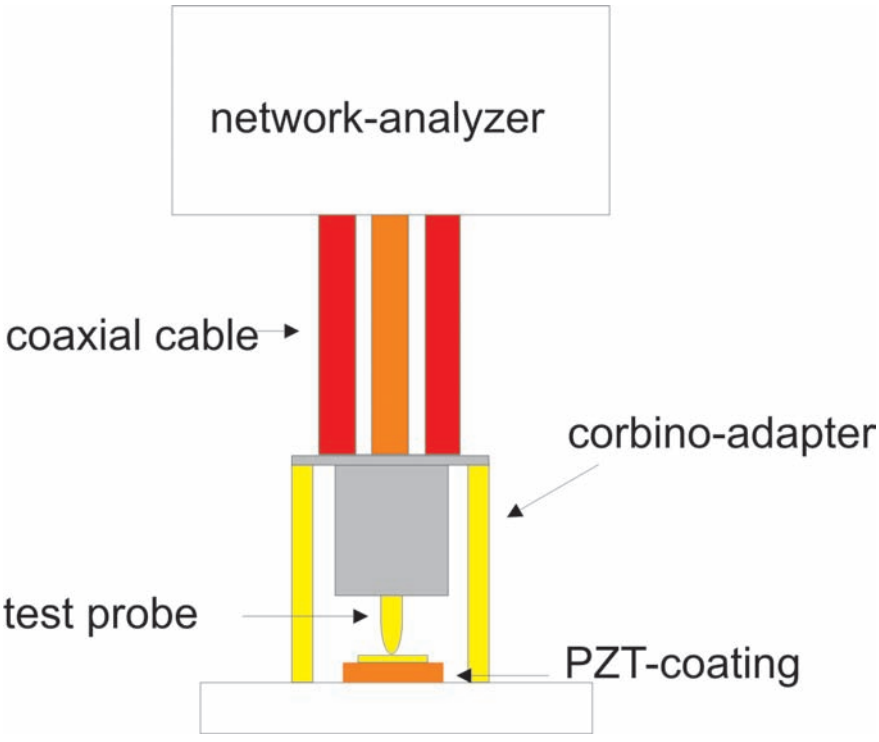


Fig. 2: Configuration for electrical characterisation of functional coatings.

The result of this measurement is the reflection factor $S_{11}$. It describes the percentage of the reflected energy at different frequencies. So a high reflection factor means a low absorption of energy by the sensor. Analysis is focused at the frequency range around the resonant frequency of the system, that depends on PZT-film- thickness.

**Results and Discussion**

In Figure 3 the X-ray patterns for mechanochemical synthesised PZT-Powder are shown. The ball-to-powder weight ratio was 20:1 and the rotation velocity was at 300 rpm. To reveal the formation of the PZT-phase, samples are taken out of the milling-jar after 15 min, 30 min, 60 min and 120 min and analyzed by X-ray-diffraction.

The phase transformation to $Pb(Zr_{0.52}Ti_{0.48})O_3$ can be observed by investigating the (120)-Peak of $PbZrO_3$ and the (100)-Peak of $PbTiO_3$. Within 120 minutes the lattices of the raw materials $PbZrO_3$ (orthorhombic) and $PbTiO_3$ (tetragonal) transform to the new lattice of $Pb(Zr_{0.52}Ti_{0.48})O_3$ (trigonal/tetragonal).

Contamination by tungsten-carbide is neither detectable by X-ray-diffraction nor by EDX. The product is a yellow PZT-powder with aggregates of 300 nm to 1 µm (Figure 4).

The measured particle size distribution confirmes the SEM-results (Figure 5).

In the following dispersion step, the PZT-powder is deaggregated in ethanol

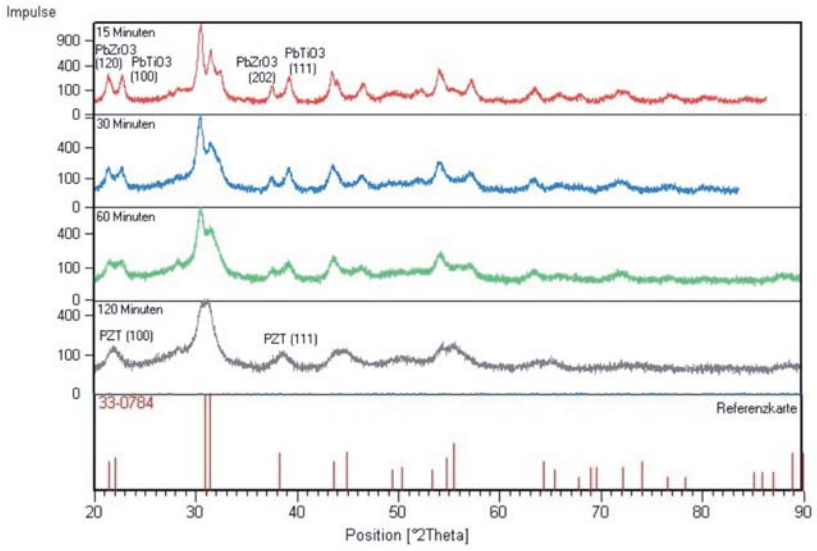


Fig. 3: X-ray-patterns of mechanochemical synthesised $Pb(Zr_{0.52}Ti_{0.48})O_3$, ball-to-powder weight ratio 20:1, 300 rpm and reference pattern for $Pb(Zr_{0.52}Ti_{0.48})O_3$.

charged with an organic surface modifier within 7 hours to a relatively narrow particle size distribution with a $d_{50}$ value of 115 nm (Figure 6).

The ζ-Potential of the modified powder shows a maximum at pH 8.5 (Figure 7), measured in ethanol. Values of pH are adjusted by NaOH and the surface modifier, an oxocarboxylic acid.

According to that, EPD is carried out at pH 8.5 adjusted by the surface modifier. The solid content in the suspension is 2 g PZT per 100 ml ethanol. Higher contents lead to cracks in the coatings, lower contents lead to porous coatings. In a similar way, the morphology of the coatings depends on deposition time. There is only a narrow working-window to get dense coatings, free of cracks. Best results are achieved with suspensions of 2 g

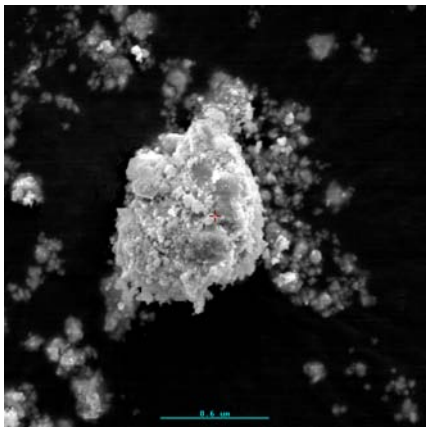

Fig. 4: SEM-image of mechanochemical synthesised PZT-aggregates.

PZT per 100 ml ethanol and deposition times between 10 and 15 seconds under an electric field of 30 V/cm. The thickness of the coatings is about 1.4 – 2 µm, depending on deposition time.

Figure 8 shows a fracture crossection of a PZT-green-film deposited on a sputtered Pt-electrode on polycrystalline $Al_2O_3$. Deposition time was 10 sec.

After deposition the green-films are rewetted with the sintering aid, a mixture of lithium acetate-dihydrate, lead acetate-dihydrate, methyl ethyl ketone and methanol. While drying, most of the solvents evaporate leaving behind the metal organics, which are then burned out during the sintering process. The films are sintered at 1050 °C for 30 min.

The average grain size, as determined by inspection of a fracture crossection of the film, is about 500 nm. The thickness of the films is about 1 µm, which corresponds to a resonance frequency at 2 GHz.

Figure 9 shows a fracture surface crossection of a sintered PZT-film on a sputtered Pt-electrode on sapphire. Top view of the coatings shows a dense crack free surface (Figure 10).

X-ray diffraction pattern for the films indicates that the films are phase pure PZT. Reactions with the substrate are not observed (Figure 11).

After sputtering the gold-top-electrode onto the PZT-films, the films are polarised by the corona method for 60 min at

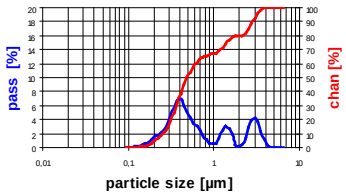


Fig. 5: Particle size distribution by volume of mechanochemical synthesised PZT-powder.

a voltage of 4 kV/cm and a temperature of 150 °C, shown in Figure 12.

Now, the completed sensors are characterised by a network analyzer. Figure 13 shows the result of the analysis. As expected, there is a resonance at 2 GHz. At that frequency nearly 80 % of the incoming energy is absorbed by the sensor-system, what relates to the oscillation of the PZT-film in thickness mode.

Figure 14 shows the top view of one of the 16 completed sensors. In the middle the gold electrode is visible. The PZT ceramic is located between the little gold electrode and a bigger platinum electrode on the sapphire. The sapphire becomes apparent by the shadow of the platinum electrode in the background. It can be observed that the PZT ceramic is transparent for visible light. This can be ascribed to a grain size of 500 nm inside the ceramic, comparable with the wavelength of visible light.

## Conclusions

Transparent crack-free PZT thin films for use in acoustic microscopy are pro-

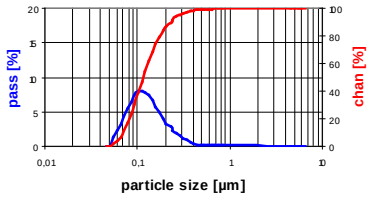


Fig. 6: Particle size distribution by volume of mechanochemical synthesised PZT-powder, dispersed in ethanol for 7 hours in a $ZrO_2$-jar.

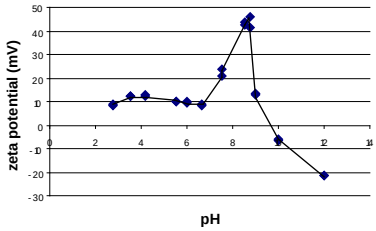


Fig. 7: ζ-potential of the synthesised PZT-powder in ethanol at various pH values.

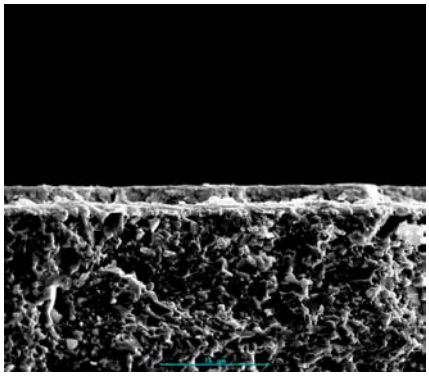

Fig. 8: Fracture surface crossection showing a PZT-green-film deposited on a sputtered Pt-electrode on polycrystalline $Al_2O_3$.

duced by mechanochemical synthesis, electrophoretic deposition and sintering of PZT-powder. As expected, the polarised films show a significant resonance at about 2 GHz.

Problems like delamination of the sputtered ground electrode were solved by using an adhesive layer.

The sinter aid, the surface modifier and the synthesised nano-powders lead to homogeneous crack-free PZT-coatings.

This work was presented at the 10th International Conference of the European Ceramic Society, June 17 - 21, 2007, Berlin and can be cited as:

M. Bender, R. Drumm, J. Adam, A. Jakob, R. Lemor, M. Veith "Preparation of Acoustic Lenses by Mechanochemical Synthesis and Electrophoretic Deposition of Lead Zirconium Titanate (PZT) Films" Proc. 10th ECerS Conf. (2007), edited by J.G. Heinrich and C.G. Aneziris, Göller Verlag, Baden-Baden, pp. 848-853.

**References**


1. Quate C.F., Atalar A., Wickramasinghe H.K.: Acoustic microscopy with mechanical scanning – A review, proceedings of the IEEE, Aug. 1979, Vol. 67, Issue: 8, 1092-1114
2. M.E. Motamedi: Acoustic Sensor Technology, Microwave Symposium Digest, 1994, IEEE MTT-S International
3. W. Tjhen, T. Tamagawa, C.-P. Ye, C.-C- Hsueh, P. Schiller, D.L. Polla: Properties of piezoelectric Thin Films for Micromechanical Devices and Systems, Micro Electro Mechanical Systems, 1991, MEMS ,91, Proceedings. ‚An Investigation of Micro Structures, Sensors, Actuators, Machines and Robots'. IEEE
4. Z. Brankovic, G. Brankovic, C. Jovalekic, Y. Maniette, m. Cilense, J.A. Varela: Mechanochemical Synthesis of PZT Powders, Materials Science and Engineering A345 (2003) 243-248
5. D. Stojanovic: Mechanochemical synthesis of ceramic powders with perovskite structure, Journal of Materials Processing Technology 143-144 (2003) 78-81
6. J. Van Tassel and C.A. Randall: Electrophoretic Deposition and Sintering of Thin/Thick PZT Films, Journal of the European Ceramic Society 19, (1999), 955-958
7. David Waller, Tariq Iqbal, Ahmad Safari: Poling of Lead Zirconate Titanate Ceramics and Flexible Piezoelectric Composites by the Corona Discharge Technique, J.Am. Ceram. Soc., 72, (1989), 2, 322-24.
8. J. Ma, R. Zhang, C.H. Liang, L.Weng: Colloidal characterization and electrophoretic deposition of PZT, Materials Letters 57 (2003), 4648-4654
9. J. Ma, Wen Cheng: Electrophoretic Deposition of Lead Zirconate Titanate Ceramics. Journal of the


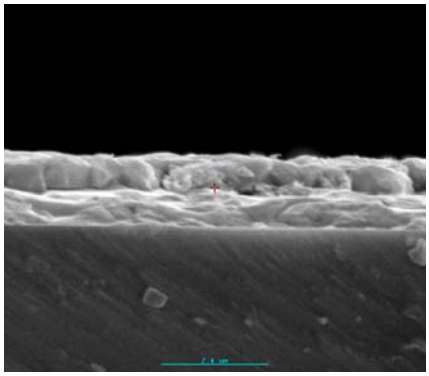

Fig. 9: Fracture surface crossection showing a sintered PZT-film on a sputtered Pt-electrode on sapphire.

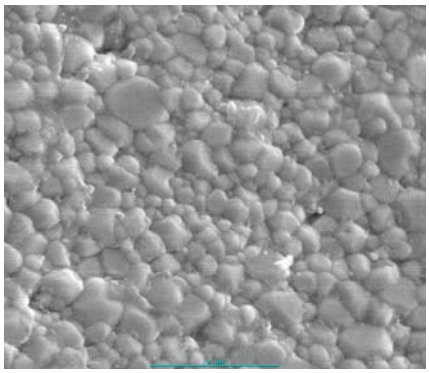

Fig. 10: Top view of a sintered PZT-coating by SEM.

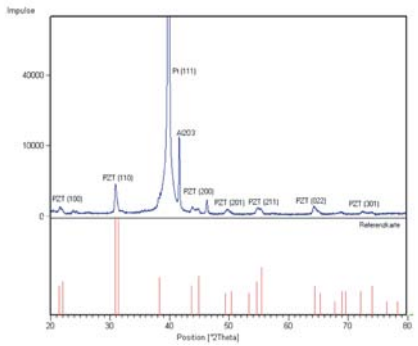


Fig. 11: X-ray diffraction pattern of a sintered PZT-film on a sputtered platinum electrode on sapphire and reference pattern for $Pb(Zr_{0.52}Ti_{0.48})O_3$

American Ceramics Society 85, 7, (2002), 1735-1737

10. J. Ma, Wen Cheng: Deposition and packing study of sub-micron PZT ceramics using electrophoretic deposition, Materials Letters 56, (2002), 721-727

11. H. Wittwer and H.G. Krüger, Möglichkeiten und Grenzen der Elektrophorese. Cfi/Ber. DKG 72, (1995), 556-560

12. B. Derjaguin, On the Repulsive Forces between Charged Colloid Particles and on the Theory of Slow Coagulation and Stability of Lyophobe Sols. Trans. Faraday Soc. 36, (1941), 203-215

13. E. J. W. Verwey and J. T. G. Overbeek, Theory of the Stability of Lyophobic Colloids The Interaction of Sol Particles having an Electric double Layer, (1948), Amsterdam-New York: Elsevier Publishing Company

## Wet Chemical Syntheses of Ag-nanoparticles

### Introduction

The synthesis of nanoparticles with well defined size, morphology and crystallinity becomes more and more important to advance in the field of nanotechnology. Especially high-temperature wet-chemical syntheses are very promising to realise the production of particles with narrow size-distribution and a sufficient yield [1-4]. Beside this goal, for industrial purposes it must be taken into account, that the chemicals costs as well as the expenses for processing are within acceptable limits. In addition, the nanoparticles have to be sufficiently stabilised to ensure their subsequent treatment. In this article, a synthesis-route for silver-nanoparticles is described which fulfils the above mentioned criteria to a large extent. Furthermore, particle size and size-distribution can be varied to some degree by changing the solvent, the heating-rate, the maximum-temperature and the duration of synthesis.

### Experimental

#### Materials

Diphenylether 99 % (DPE), dibenzylether 99 % (DBE), dioctylether 99 % (DOE), 1-hexadecene 92 % (1-HD) and oleic acid 90 % (OA) were purchased from Aldrich, 1-octadecene 90 % (1-OD) from Alfa Aesar, 1-eicosene 85 % (1-Eic) from ABCR, tri-n-octylamine 98 % (TNO) from Acros, silver nitrate 99 % ($AgNO_3$) and oleylamine 70 % (OAA) from Fluka. All chemicals were used without further purification.

#### Syntheses

#### Synthesis route 1

In a typical synthesis, 10 ml solvent (for example DBE) and 8 mmol (2.26 g) OA were mixed in a 100 ml three-necked

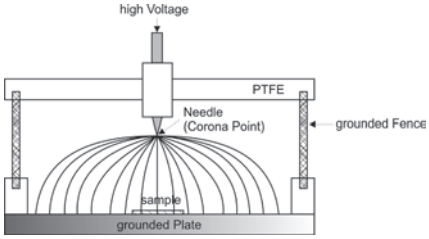


Fig. 12: Polarisation by the corona method

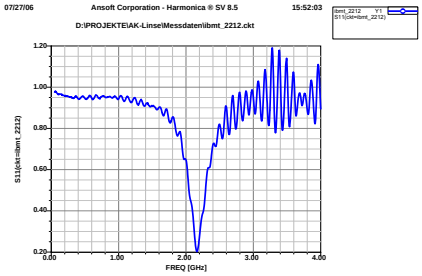


Fig. 13: Dependence of the reflection factor S 11 of various frequencies

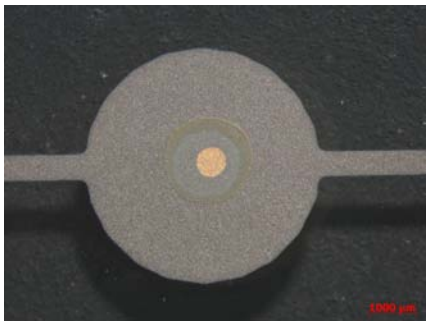

Fig. 14: Completed sensor, image made by light-optical microscope